



Published in final edited form as:

Drug Resist Updat. 2011 ; 14(4-5): 224–235. doi:10.1016/j.drug.2011.04.004.

Translational imaging endpoints to predict treatment response to novel targeted anticancer agents

Natalie J. Serkova, PhD

Departments of Anesthesiology and Radiology, University of Colorado Cancer Center, Animal Imaging Core, University of Colorado Denver, Anschutz Medical Center, Aurora, CO 80045, USA

Abstract

Response Evaluation Criteria in Solid Tumors (RECIST) and World Health Organization (WHO) Criteria have been traditionally used for the evaluation of therapeutic response to chemotherapeutic treatment regimens. They determine anatomic criteria for patients response to anti-cancer therapy based on morphological measurements of each target lesion. While this assessment is justified for cytotoxic (chemotherapeutic) drugs, it is now recognized that morphological imaging protocols are poorly suited to the evaluation of the efficacy of novel signal transduction inhibitors (STIs) which exhibit cytostatic rather than cytotoxic properties. New imaging technologies are now designed to evaluate, in a functional manner, modifications in tumor metabolic activity, cellularity, vascularization before a reduction in tumor volume can be detected. Introduction of physiological imaging end-points, derived from dynamic contrast-enhanced (DCE) imaging protocols – including magnetic resonance imaging (MRI), computed tomography (CT) and ultrasound (US) - allow for early assessment of disruption in tumor perfusion and permeability for targeted anti-angiogenic agents. Diffusion-weighted MRI (DWI) provides another physiological imaging end-point since tumor necrosis and cellularity are seen early in response to anti-angiogenic treatment. Changes in glucose and phospholipid turnover, based on metabolic MRI and positron emission tomography (PET), provide reliable markers for therapeutic response to novel receptor-targeting agents. Finally, novel molecular imaging techniques of protein and gene expression have been developed in animal models followed by a successful human application for gene therapy-based protocols.

Keywords

functional imaging; magnetic resonance imaging; positron emission tomography; signal transduction inhibitors; contrast enhanced imaging; personalized medicine

1. Introduction

In vivo biomedical imaging involves administering a known amount of energy to the body and measuring, with spatial localization, the energy that is transmitted through, emitted from, or reflected back from various organs and tissues (Brindle, 2008). The energy most

© 2011 Elsevier Ltd. All rights reserved.

Address for Correspondence: Dr. Natalie J. Serkova, Associate Professor Department of Anesthesiology, University of Colorado Denver, Anschutz Medical Center 12631 East 17th Avenue; Mail Stop 8202; Aurora, CO 80045 (phone) 1 303 724 1086; (fax) 1 303 724 1761 Natalie.Serkova@UCDenver.edu.

Publisher's Disclaimer: This is a PDF file of an unedited manuscript that has been accepted for publication. As a service to our customers we are providing this early version of the manuscript. The manuscript will undergo copyediting, typesetting, and review of the resulting proof before it is published in its final citable form. Please note that during the production process errors may be discovered which could affect the content, and all legal disclaimers that apply to the journal pertain.

commonly used is some form of electromagnetic energy, such as X-rays or lights, but occasionally other forms are used such as mechanical energy for ultrasound scans. Imaging the human body began as part of routine clinical care with the development of X-ray imaging by Roentgen (Serkova et al., 2009). Computerized tomography (based on 3D X-ray scan representation) has added immeasurably to the ability to find, measure, and monitor pathologies. The algorithms originally developed by Hounsfield to produce tomographic images with X-rays have also been extended to nuclear medicine for use with positron emission tomography (PET) and single photon emission computed tomography (SPECT). The development of magnetic resonance imaging (MRI) has provided high levels of contrast with superb resolution in many areas of the body. These modalities have been complemented by ultrasound (US) imaging and more recently by the introduction of new optical imaging (OI).

The major advantage of all imaging technologies includes their non-invasive nature in addition to their translational capabilities. Indeed, as of today, all imaging modalities exist for clinical and preclinical applications (with the exception of optical imaging which mostly remains in preclinical animal application). Applying imaging modalities in small animals allows for acceleration in the development of new imaging markers and drugs as well as increase in our understanding of pathophysiological processes. Imaging in mice is important because of the widespread use of genetically engineered mice in biomedical research and the need to measure the *in vivo* anatomic, functional and molecular phenotypes. Animal imaging is highly attractive because the *in vivo* environment can be successfully captured (*in vivo* \neq *ex vivo*); it is non-destructive (each animal serves as its own control); it can efficiently survey the whole animal and, finally, it provides a translational bridge from animal to human studies (Weissleder and Mahmood, 2001; Gambhir, 2002). Advanced technologies developed for imaging in small animals are identical to human imaging modalities and, therefore, can generally be translated directly for application in clinical scanners. Therefore, oncologic imaging represents a sophisticated area which can provide researchers and clinicians with reliable *in vivo* endpoints for assessment of cancer progression, efficacy of novel anti-cancer agents as well as resistance development. These imaging end-points deliver quantitative information on tumor size, presence or absence of metastases, physiology and metabolism, as well as, more recently, on molecular markers and targets of specific malignancy, thereby providing a possibility for personalized medicine.

In the past decade, the practice of oncology has evolved from the exclusive use of cytotoxic compounds that non-selectively inhibit cells actively engaged in the cell cycle to include newer targeted agents (signal transduction inhibitors, STIs) that can block particular pathways important for neoplastic transformation, growth, and metastasis. Without being truly cytotoxic (no immediate cell death) but rather cytostatic, it is increasingly important to apply sensitive quantitative imaging end-points to monitor therapy response. The present review provides insights into existing imaging technologies and the development of novel imaging protocols to establish functional pharmacodynamic imaging end-points to assess patient response to novel targeted therapies (Spratlin et al., 2010; Nayak et al., 2011; Mileshkin et al., 2011; Zander et al., 2011; Pope et al., 2011; Krause et al., 2011). New imaging technologies are now designed to evaluate, in a functional manner, modifications in tumor metabolic activity, cellularity and vascularization before a reduction in tumor volume can be detected.

2. Imaging technologies for physiological, metabolic and molecular imaging

In order to take full advantage of existing imaging modalities for establishing comprehensive anatomical, physiological and metabolic end-points, one needs to understand

basic underlying principles of physics for each modality. As mentioned above, all imaging modalities are based on physical phenomena which involve interaction of external energy in form of radiofrequency waves (MRI), X-rays (CT), radiation decay (PET, SPECT) or sound waves (US) with the human or animal body in order to spatially and time-dependently reconstruct anatomical, physiological or molecular images. Here a brief summary is provided on how major imaging modalities function.

2.1. Magnetic Resonance Imaging and Spectroscopy (MRI and MRS)

MRI generates images by applying an external varying magnetic field to the body. MR is probably the most complex technique in the field of medical physics. The magnetic field aligns hydrogen atoms parallel and anti-parallel to the magnetic field. When a signal in the form of a radio wave-pulse is applied to the body using surface coils, atomic distribution between parallel and anti-parallel alignment is changed, and after the pulse is gone, the system relaxes to its original status (Tidewell and Jones, 1999; Lauterbur, 2004; Mansfield, 2004). Hydrogen atoms in different tissues have different relaxation properties which can be detected by radio-frequency MR receivers. MRI of tissue relaxation characteristics following a radiofrequency pulse of energy can be then translated into information about the concentration, mobility, and chemical bonding of hydrogen and, less frequently, other tissue elements. Although many other MRI techniques exist, the two basic types of images are T1- and T2-weighted MRI (**Figure 1A**). T1-weighted images show fat as a white bright signal, whereas water and cerebrospinal fluid (CSF) are dark. On a T2-weighted image, fat is gray, and blood, edema, and CSF appear white. Unfortunately, calcification is difficult to see on MR images. In addition to anatomical imaging, a physiological assessment of organ perfusion and permeability can be made by injection of gadolinium-based agents and calculation of their uptake into the organ of interest on T1-weighted images (**Figure 1B**) (Hylton, 2006). The use of iron-oxide-based nanoparticles (super-paramagnetic iron oxide, SPIOs, and ultra-super-paramagnetic iron oxide, USPIOs), on the other hand, allows for molecular imaging based on T2-weighted scans (**Figure 1C**) (Serkova et al., 2010). Using relaxation properties of other hydrogen-containing endogenous molecules or other atoms (such as ^{31}P and ^{13}C), metabolic information can be obtained non-invasively in a magnetic resonance spectroscopy (MRS) scan (Gillies and Morse, 2005; Leach, 2006). MRS can be based on observation of protons in various metabolites (such as ^1H -MRS of citrate in prostate cancer; ^1H -MRS of choline in breast, prostate and brain cancer; ^1H -MRS on N-acetyl aspartate and myo-inositol in brain cancer) or phosphorus metabolites by ^{31}P -MRS (membrane phospholipids in tumors, or ATP and phosphocreatine in the muscle) (**Figure 1D**). In general, MRI is the method of choice for imaging the central nervous system, musculoskeletal system and stationary soft tissues. There is limited applicability of MR for imaging of lungs. However, one of the most recent discoveries related to MR application in the lung, namely the use of hyperpolarized ^{129}Xe or ^3He gas for imaging of pulmonary gas transfer, allows a clinician or image recognition program to assess gas exchange and/or alveolar-capillary barrier status in the lung (Deppe et al., 2011). Most recently, carbon hyperpolarization (as, for example, hyperpolarized pyruvate) allows for fast and sensitive *in vivo* assessment of cancer metabolism (Kurhanewicz et al., 2011) – however, this technique is still in its infancy and demands further technological developments. **Advantages of MRI:** Superior spatial resolution, great soft tissue contrast, no ionizing radiation, establishing anatomic, metabolic, physiological and molecular imaging end-points.

Disadvantages of MRI: one of the most expensive and technically most challenging imaging modalities, long scan times for large volume/ high resolution.

2.2. X-ray and Computed Tomography (CT)

In biomedical imaging, X-ray techniques, including CT, can reveal intrinsic properties of an object such as its physical and electron density. The X-rays are absorbed in different amounts by the various tissues or materials in the body. Most of the beam is absorbed or scattered, however a small percentage of the beam exits the patient and strikes a detector (Vaughan, 2007). CT images are acquired with an X-ray tube passing a rotating fan beam of X-rays through the body and measuring the transmission at thousands of points with detectors. CT scans are presented as a series of slices of tissue, and the computers can then display the data as a three-dimensional rotating image. Compared with plain X-rays, CT uses 10 to 100 times more radiation. The appearance of tissue on CT scan can be divided into the four basic densities: air is black, fat is dark gray, soft tissue is light gray, and bone or calcium and contrast agents are white (**Figure 2**). Therefore, CT protocols are superior for bone and lung scans. CT is currently one of the most commonly used imaging modalities given faster scanner, widespread availability and high spatial resolution. However, CT has relatively poor contrast resolution in comparison to MRI. This limitation can be partially overcome by the use of contrast agents.

Advantages of CT: high spatial resolution, whole body 3D-coverage, moderate costs, short scans.

Disadvantages of CT: high radiation dose, mostly anatomic information, poor soft tissue contrast.

2.3. Positron Emission Tomography (PET)

Nuclear medicine images are produced by giving the patient short-lived radioactive isotopes and detecting their decay by a gamma camera or positron emission scanner. Nuclear medicine procedures, including PET and SPECT, reveal spatial and temporal distribution of target-specific radiotracers and pharmaceuticals. In PET, a positron-emitting radioisotope is administered in very small doses (usually less than 0.3 mCi for a mouse and less than 20 mCi for a patient) intravenously and the distribution of the tracer is imaged (Gambhir, 2002; Kapoor et al., 2005). Depending on the application, these data can be interpreted to yield information about properties such as glucose metabolism, blood volume and flow, tissue uptake, receptor binding, and oxygen utilization. Although an extensive array of different radiopharmaceuticals, or molecular probes (including carbon 11, nitrogen 13, oxygen 15 and fluorine 18 based tracers), to image different aspects of pathophysiology and biology are available for PET imaging, the most widely used, and the only clinically approved PET tracer is the fluorinated analogue of glucose, ¹⁸fluorine-2-deoxy-D-glucose (¹⁸FDG). The increased uptake of glucose in malignant cells has been known for many years (first described by Otto Warburg in 1930), and the high-uptake of FDG can be used to detect tumor lesions and metastases (Kapoor et al., 2005a). There is physiological FDG uptake by brain, heart, kidney and bladder and, in mice, by brown fat on FDG-PET (Fueger et al., 2006). The major advantage of PET is its ability to assess molecular function; however, PET is limited by poor spatial resolution making it difficult to accurately localize FDG uptake to an anatomical structure. This limitation has been significantly reduced by combining PET with CT, a technique in which both PET and CT are performed sequentially during a single visit on a hybrid PET/CT scanner (**Figure 2**). The PET and CT images obtained are co-registered using fusion software, thereby enabling accurate designation of physiologic and molecular data obtained on PET to anatomic structures visualized on CT (Blodgett et al., 2007). PET/MRI has also been recently explored in animal imaging. In general, PET is a method of choice for physiologic and biochemical information; however, PET studies require radiation exposure. Additionally, a cyclotron facility is required to produce the ultrashort half-life of isotopes making this imaging modality relatively expensive.

Advantages of PET: high sensitivity (nM-pM), labeling of small molecules with little or no change in biological action, whole body 3D-volumetric imaging, quantitative, straightforward translation from mouse to man.

Disadvantages of PET: involves ionizing radiation, access to radiolabeled molecules, especially for short half-life radionuclides (need for cyclotrons), lower spatial resolution.

2.4. Ultrasound (US)

Ultrasound uses high-frequency sound waves to make images. Ultrasound image is created with the capture of ultrasound energy reflected from interfaces in the body (“echoes”) that separate tissue with different acoustic impedances, where the acoustic impedance is the product of physical density and velocity of sound in the tissue (Bolondi et al., 2007). Typically, a cyst appears sonolucent because it has a few if any echoes (because it is mostly water), while liver and spleen have solid homogenous echo texture due to medium level echoes from the fibrous interstitial tissues. High-intensity echoes (increased echogenicity) are caused by calcification, fat and air. The technology of ultrasound is attractive because it does not use ionizing radiation, can produce real-time image and is less expensive than any other modality (Blomley and Eckersley, 2002).

Advantages of US: real-time, no ionizing radiation, low cost, good spatial resolution, physiological information.

Disadvantages of US: requires direct contact with animals, limited field of view.

2.5. Optical Imaging (OI)

OI modalities utilize highly sensitive detectors for bioluminescent or fluorescent light that is transmitted through tissues from internal sources. Optical filters can select both excitation and emission wavelength (Weissleder and Ntziachristos, 2003). In fluorescence imaging, excitation light in the visible region (400-600 nm) is used to excite fluorophores in the tissue, which emit fluorescence at longer wavelengths. Bioluminescence imaging relies on the genetic engineering of tissues to express luciferases. These are photoproteins, isolated from organisms such as the firefly, which modify their substrates and in so doing produce light, which can be detected using sensitive device cameras. The advantage over fluorescence imaging is that bioluminescence is very sensitive, as there is no background, with detection sensitivity of $10^{-7} - 10^{-5}$ M. Both techniques are limited by the low depth of penetration (1-2 mm) due scattering and absorption of the emitted photons. They are not really quantitative either. As of today, bioluminescence is exclusively used in mice for molecular imaging.

Advantages of OI: accessible inexpensive technology, low cost with high-throughput, highly sensitive for targets, activatable contrast agents, no ionizing radiation.

Disadvantages of OI: difficult to translate to man, 3D challenging, not quantitative, contrast agents for protein targeting can be limited by size of fluorophores.

Each of the imaging technologies has its own advantages and disadvantages (see above) in spatial resolution, functional assessment and in imaging of molecular targets. When assessing strengths and weaknesses of each modality, the following important image characteristics should be taken into account (summarized in **Table 1**):

- Spatial resolution: what is the smallest object I can visualize?
- Signal-to-noise: what is the precision of the measurement?

- Quantitation: what is the accuracy of the measurement?
- Contrast-to-noise: what differential in image intensity must I have to be able to visualize an object of interest?
- Sensitivity: what concentration of a tracer, probe or contrast agent must I have to be able to detect an object?

2.6. Contrast Agents (CAs)

Injectable tracers are available for each modality mostly for enhancing tissue and/or lesion contrast. They are also used to obtain dynamic functional information of tissue/lesion perfusion and permeability (such as dynamic contrast-enhanced DCE-MRI, CE-CT or CE-US). For nuclear medicine and bioluminescence, radioactive and luciferase-containing tracers are required for detecting a signal (no background signal is available) (Hasebroock and Serkova, 2009; Dobrucki et al., 2010).

- CT CAs: Intravenous, oral or rectal (mostly iodine-based) contrast agents are used for CT. Iodinated contrast media are routinely used to enhance x-ray and CT images for neoplastic lesion detection, angiography for coronary disease and dynamic perfusion studies. For molecular imaging, there are attempts to use gold nanoparticles.
- MRI CAs: Two major classes, (i) Gadolinium (Gd)-based chelates (paramagnetic) reduce T1 relaxation times resulting in increasing brightness of T1-weighted images; (ii) Iron-oxide nanoparticle based (SPIO, USPIO) superparamagnetic agents, which reduce T2 relaxation times with decreasing signal intensity on T2-weighted images. Gd-chelates: magnevist, omniscan, multihance. SPIO: feridex, resovist.
- PET CAs: they are radiolabeled short-life molecules, peptides, antibodies. Most of the time they need to be produced on-site (half-life times: ^{18}F 110 min; ^{11}C 20 min; ^{13}N 9.9 min; ^{15}O 120 sec).
- US CAs: gas or air-filled microbubbles or lipid microspheres are used which are strong scatterers of US: optison, definity, levovist, echogen, biosphere are intravascular; SonoRx is used orally.
- OI CAs: they are mostly fluorescent proteins = enzymes, which catalyze the bioluminescent reaction or fluorescent molecules/ dyes used to label biomolecules and cells.

New targeted agents (including PET radiotracers, MRI nanoparticles and luciferase constructs) are designed to visualize genes (Weissleder and Mahmood, 2001), proteins (Serkova et al., 2010), tumor pH and microenvironment (Zhang et al., 2010).

3. Oncologic imaging for assessment of therapy response

New therapeutics in oncology are increasingly designed to specifically target aberrant pathways involved in tumor growth, proliferation and metastasis. Biomarkers are being increasingly utilized in the early clinical development of such agents to identify, validate and optimize therapeutic targets and agents, to determine and confirm mechanism of drug action and as a pharmacodynamic endpoint to predict or monitor the responsiveness to treatment, toxicity or resistance (Evelhoch et al., 2005). Moreover, many of the newer agents act in a cytostatic rather than cytotoxic (cell kill) manner. The Response Evaluation Criteria In Solid Tumors (RECIST) and World Health Organization (WHO) Criteria have been traditionally used for the evaluation of therapeutic response to cytotoxic chemotherapy regimens (Jaffe, 2006; Jaffe, 2008). They determine anatomic criteria for patients response

to anti-cancer therapy based on morphological measurements of each target lesion. While this assessment is justified for cytotoxic drugs, it is now recognized that morphological imaging protocols are poorly suited to the evaluation of the efficacy of novel signal transduction inhibitors (STIs) which exhibit cytostatic rather than cytotoxic properties. Thus, for the oncologist, additional drug effects than anatomical tumor shrinkage may be important and novel, physiological imaging end-points can provide an informative contribution to estimate early therapy response and/or resistance development.

3.1. Cytotoxic and cytostatic anticancer agents

Cytotoxic anticancer agents are used for the initial treatment of several types of solid tumors as well as in the neo-adjuvant and adjuvant setting and in palliative care. The primary mechanism of action of chemotherapeutic agents is perturbation of the cellular processes involved in proliferation: DNA synthesis and cell division. These effects often result in cell death by either apoptosis or necrosis (Kerbel and Kamen, 2004; Brunelle and Zhang, 2010).

Tumor growth, angiogenesis, invasion and metastasis are largely regulated by growth factor signaling via their cognate receptor tyrosine kinases. Inhibition of these signaling pathways as a therapeutic approach has recently gained a lot of attention (Levitzki and Gazit, 1995; Hollande et al., 2010). Accordingly, many novel targeted agents are signal transduction inhibitors (STIs) including anti-growth factor antibodies, anti-receptor monoclonal antibodies, anti-sense and small molecule tyrosine kinase inhibitors (Levitzki and Gazit, 1995; Dancey and Sausville, 2003), starting with the introduction of imatinib, which targets BCR-ABL and Kit, for the treatment of chronic myeloid leukemia (Druker et al., 2001) and now including agents targeting VEGF, VEGFR2, EGFR (erbB1), erbB2 (Her2), IGF1R as well as major downstream signaling kinases MEK, Raf, Akt and mTOR (Dent et al., 2009; Zhang et al., 2011).

Unfortunately, similar to traditional chemotherapy, development of resistance has become a major problem for targeted anti-cancer therapies (Broxterman et al., 2009). In the setting of breast cancer for example, most patients with metastatic disease receiving trastuzumab-containing regimens experience disease progression within one year, with salvage chemotherapy effective in about 10% of cases. A variety of resistance mechanisms to trastuzumab are postulated (Nahta and Esteva, 2007; Zhang et al., 2011). To date there has been little clinical success with re-instituting sensitivity to anticancer drugs once resistance emerges, while functional imaging could contribute significantly to prediction of the patient response to therapy. The Food and Drug Administration (FDA) has targeted imaging as a tool to help in translational and clinical drug development (Evelhoch et al., 2005). Functional and molecular imaging – especially MRI and PET – are assigned by the FDA to better delineate the end-points of therapy response.

3.2. Morphological assessment of cytotoxic treatment

RECIST and WHO criteria, which are currently the most widely used criteria for the evaluation of anti-tumor cytotoxic therapies, are based on morphological measurements of each target lesion. Until now, the tumor response or objective response has been based on changes in the number and size of measurable primary or secondary target lesions (Jaffe, 2006, Jaffe, 2008; Eisenhauer et al., 2008; Ramasamy et al., 2011). Besides RECIST evaluations (mostly derived from CT scans), diffusion-weighted (DW)-MRI is used to assess tumor necrosis which is caused mostly by chemotherapeutic cytotoxic agents and, to a lesser extent, by anti-angiogenic regimens. In DW-MRI, the motion of water molecules in the tissue is detected from the additional changes in their physical properties as the molecules diffuse through the cell membrane (Koh and Collins, 2007). Because free diffusion of protons is inhibited by cell membranes, DW-MRI can sensitively detect

deteriorations in cell membranes and, therefore, cellular injury. Most tumors show increased cellularity and reduced water diffusion (hypodensity signal in DW-MRI) frequently attributed to increased proliferation and cell density in tumors. Tumor cellularity can then be quantitatively assessed by comparing apparent diffusion coefficients (ADCs) from malignant areas to the ADCs of normal tissues (Desouza et al., 2007; Reinsberg et al., 2007). After cytotoxic treatment, a significant increase of ADC coefficients can be seen reflecting an increase in proton diffusion and decreased cellularity or necrosis development (**Figure 3**) (Padhani et al., 2009; Rozel et al., 2009; Thoeny and Ross, 2010). Finally, a decrease in tumor T1 relaxation times reflects hypocellularity and necrosis and can be introduced as a quantitative imaging end-point in clinical trials based on cytotoxic agents (McSheehy et al., 2009).

3.3. Imaging anti-angiogenic treatment

The microvasculature of tumors, in contrast to normal tissue, is structurally and functionally abnormal, tortuous and poorly organized, making the vessels “leaky” (Jain, 2003) and it has been identified as a rational target for cancer therapy (Folkman, 1990). Dynamic contrast-enhanced (DCE)-MRI can be used for the non-invasive assessment of tumor vascular properties (Hylton, 2006; Barrett et al., 2007; Thomassin-Naggara et al., 2008). DCE-MRI is based on fast T1-weighted dynamic MRI scans prior and during gadolinium contrast injection. Given that hypoxic tumors are resistant to radiation and chemotherapy and that heterogeneous tumor blood flow may affect the efficacy of systemic chemotherapeutics, methods for assessing tumor blood flow or perfusion characteristics, as a marker of hypoxia, may help clinicians to predict the response or adapt or select a more aggressive alternative therapeutic approach (Semple et al., 2006; Zahara et al., 2007). Furthermore, with the increasing use of anti-angiogenic agents, that may not cause dramatic reduction in tumor volume, DCE-MRI can provide a quantitative method of monitoring and characterizing treatment response (Robinson et al., 2003; Marzola et al., 2004; Troiani et al., 2007; Moasser et al., 2007; Barrett et al., 2007; Spratlin et al., 2010). The ability of DCE-MRI to quantify a range of characteristics of tumor microvasculature based on enhancement in T1-weighted images has encouraged many investigators to use this technique as a basis for *in vivo* staging of tumors and therapy response (**Figure 4**). Correlation of DCE-MRI based features of tumor microvasculature with pathology, therapeutic response and prognosis remains the main goal for future work with these techniques (Leach et al., 2005). Several preclinical and clinical studies have been published illustrating the utility of DCE-MRI to show microvascular changes as a result of anti-VEGF or VEGFR targeted therapies; the response (decreased gadolinium uptake) can be seen as early as 2 weeks of the treatment, before tumor regression (Morgan et al., 2003; Liu et al., 2005; Troiani et al., 2007; Spratlin et al., 2010).

Similarly to DCE-MRI, quantitative contrast-enhanced (CE)-CT based on time-dependent contrast enhancement after injection of iodine-based contrast agents can be performed (Miles et al., 2007). Due to some technical limitation as well as potential toxicity of CT-contrast agents, CE-CT is less accepted than DCE-MRI, even though kinetic modeling on CE-CT yields similar results as from gadolinium kinetics (Bisdas et al., 2008).

Early evaluation using contrast-enhanced ultrasound (using microbubbles) also has been applied with success to gastrointestinal stromal tumors (GISTs) and kidney tumors. It allowed prediction of the response to treatment, characterized by a 20% reduction in contrast agent uptake after one week of treatment in GISTs (Lassau et al., 2006) and fifteen days of treatment in kidney cancer. It has been demonstrated that these response criteria are accompanied by a significant difference in progression-free survival (Lamuraglia et al., 2006; Escudier et al., 2007; Lassau et al., 2007). Contrast-enhanced ultrasound with qualitative analysis has existed for more than 5 years in clinical practice. It has also been

utilized to image neovascularity in primary prostate cancers (Halpern, 2006; Padhani et al., 2005). It is now coupled with the use of second-generation contrast agents combined with perfusion software (Greenbaum et al., 2007; Turnbull, 2009). It is now possible to acquire raw data proportional to the real response of microbubbles generated by the contrast agents (linear raw data) detected by the ultrasound probe (Wilson et al., 2009; Wilson and Burns, 2010). These linear data make it possible to assess with precision the actual perfusion of the tumors and to calculate parameters characterizing the perfusion, thus allowing quantitative analysis.

3.4. Metabolic response to anticancer agents

The dominant modality for imaging tumor biochemistry and physiology *in vivo* is PET. Because most malignancies exhibit increased glucose uptake and glycolytic metabolism, the majority of clinical PET studies are based on intravenous injection of ^{18}F FDG, which is a marker for hexokinase activity (the rate-limiting step in glucose metabolism). Glucose dependence in various malignancies relies on overexpression of glucose transporters (mainly GLUT-1) and key enzymes of glycolytic pathways, such as hexokinase, pyruvate kinase, and phosphofruktokinase. Hence, ^{18}F FDG is transported into the cell by the energy-independent GLUT-1 transporter. Unlike the natural glucose, however, FDG is trapped inside the cell because it cannot be metabolized by glucose-6-phosphate isomerase (Gambhir et al., 2001) and is accumulated in cancer cells which have high expression and activity of GLUT-1.

Several studies have suggested that FDG-PET (with hybrid PET/CT becoming more and more prevalent for metabolic imaging) may be used to monitor drug response very early in the course of therapy (Shankar et al., 2006). A quantitative change in tumor FDG uptake 2-3 weeks after start of therapy has been shown to correlate with subsequent tumor shrinkage and patient survival (Weber, 2005; Weber and Figlin, 2007; Castell and Cook, 2008). A decrease in FDG uptake as an assessment of therapy response has been seen in patients with head and neck carcinoma, lymphoma, breast, lung and colorectal cancer (Kostakoglu and Goldsmith, 2004; Kapoor et al., 2005a; Kapoor et al., 2005b; Na et al., 2008; Evilevitch et al., 2008; Leibold et al., 2011). A complete response in FDG-PET was defined as normalization of a PET scan without abnormal FDG uptake and partial response as a significant reduction in FDG uptake of all known lesions without the appearance of new lesions. A metabolic response in PET has been defined as decrease of SUV (standard uptake values) of the primary tumor by at least 20%. Recent studies have shown that radiation, chemotherapy as well as targeted treatment induces changes in tumor FDG uptake (see **Figure 5**) and residual FDG uptake after completion of therapy are highly significantly correlated with inhibition of tumor growth in animals and with patient survival in clinical studies (Na et al., 2008). For the majority of tumors, metabolic PET was superior to CT in radiotherapy planning and assessment of therapy response (Gregoire et al., 2007). Several studies have indicated that in responding tumors, FDG uptake markedly decreases within the first chemotherapy cycle or after 14 days of treatment (Kostakoglu et al., 2006; Evilevitch et al., 2008; Lippert et al., 2011; Leibold et al., 2011). In gastric cancer patients treated with chemotherapy, metabolic responders by PET also showed a high histopathologic response rate (69%) and favorable prognosis, whereas metabolic non-responders have a poor prognosis and showed histopathologic response in only 17% (Ott et al., 2008). The metabolic response to targeted drugs, such as imatinib in gastrointestinal stromal tumor (GIST) patients, can occur in the first hours after treatment begins and can be used to adjust a patient's daily dose (Hughes et al., 2004). Even in hepatocellular carcinoma patients, known to have low FDG uptake on liver PET scans at the baseline, after 3 weeks of sorafenib treatment (a multitargeted VEGFR2 STI) a partial metabolic response was clearly

seen in a responder versus non-responder (Siemerink et al., 2008). Pre-clinically, glucose metabolic activity closely reflected response to the EGFR STI gefitinib (Su et al., 2006).

The potential uses of clinical PET in oncology are far reaching and extend beyond the imaging of glucose metabolism. [¹⁸F]-labeled thymidine (3'-deoxy-3'-(¹⁸F)fluorothymidine, FLT) is a PET radiotracer which is used for non-invasive imaging of tumor proliferation since its uptake is directly related to DNA synthesis (Leyton et al., 2005) and can provide a sensitive marker for effects of DNA-disrupting agents as shown for cisplatin (Leyton et al., 2005).

In addition, novel radiotracers, related to various metabolic abnormalities in cancer metabolism, are currently under development. For example, the use of technically improved PET/computed tomography scanners with new tracers like ¹¹C and ¹⁸F choline and acetate might offer better assessment of recurrent prostate cancer than FDG-PET (Pucar et al., 2008).

Additional metabolic modalities, MRS and MRSI, can also serve as putative quantitative biomarkers for therapy response (Galbraith, 2006). In prostate cancer patients after radiation therapy, MRI and MRS (based on quantitative choline, creatine and citrate sets) showed estimated sensitivities of 68% and 77%, respectively, for therapy response, while sensitivities of biopsy and digital rectal examination were 48% and 16%, respectively (Pucar et al., 2005).

3.5. Molecular imaging for therapeutic response

A new and important imaging application in molecular medicine is the use of imaging tracers to study molecular and genetic processes. The field of molecular imaging has been defined as the non-invasive, quantitative and repetitive imaging of biomolecules and biological processes in living organisms. For example, cancer cells may be genetically altered to attract molecules that (i) alter the magnetic susceptibility, thereby permitting their identification by MRI; or (ii) decay with emission of radiation that can be detected externally by PET or SPECT; or (iii) by introducing specifically engineered cells containing luminescent or fluorescent reporters to visualize them by optical imaging.

Molecular imaging probes provide the imaging signal and are composed of an affinity component that interacts with the target and a signaling component that is useful in imaging. For PET, the imaging compound is a radioisotope; in MRI it can be SPIO nanoparticle or gadolinium; in optical imaging, it is usually a fluorochrome (Massoud and Gambhir, 2003).

PET is ideally suited for molecular imaging due to its high sensitivity, lack of the background signal and the ability to replace one chemical moiety of a ligand with a radioisotope (Gambhir, 2002). Some initial studies include ⁶⁴Cu-labeled octreotide and ⁶⁸Ga-labeled octreotide analogues for targeting somatostatin-receptor-positive tumors (Anderson, 2001; Henze, 2001). A clinical study reported on the successful use of [¹⁸F]galacto-RGD PET in patients with head and neck carcinoma in order to scan integrin $\alpha\beta 3$ expression, a receptor involved in angiogenesis and metastases (Beer et al., 2007). Recently, ⁸⁹Zr-ranibizumab was used to show as a VEGF-PET based imaging to show the efficacy of sunitinib treatment in mouse xenograft models of human cancer (Nagengast et al., 2011).

Magnetic resonance is a particularly attractive modality for molecular imaging due to the ability of MR instruments to acquire high-resolution anatomical images. Active targeting of SPIO or gadolinium-based nanoparticles provides a means to image molecular targets. For tumor site imaging, this requires that the target of interest is overexpressed or expressed

exclusively or selectively on tumor cells. The transferrin receptor, which is overexpressed on cancer cells, is one of the examples. SPIO nanoparticles conjugated to transferrin, which binds to the transferrin receptor, accumulate in the tumor following transferrin-receptor mediated endocytosis and produce a 40% change in T2-signal intensity (Hogemann et al., 2000). Clinically relevant, overexpression of the Her-2/ neu tyrosine kinase receptor and efficacy of Herceptin treatment in breast cancer can be visualized after injection of SPIO–herceptin conjugate (Artemov et al., 2003). Myofibroblast infiltration into implanted ovarian carcinoma spheroids was followed by MRI or optical imaging after labeling myofibroblasts with various molecular reporters in mouse models (Granot et al., 2007).

Finally, optical imaging (OI) in preclinical studies also allows for visualization of target proteins and genes. VEGF expression was targeted with an anti-VEGF antibody conjugated with a fluorescent dye. OI successfully images VEGF levels quantitatively in different tumors and showed concordance with ELISA results (Chang et al., 2008). OI techniques have been used increasingly for the detection of gene expression and assessment of treatment response in experimental animals. Bioluminescence can reveal both the gene transfer to tumors and the subsequent therapy-induced reduction in transgene expression. The suicide and reporter gene HSV1-tk has been studied intensively (first preclinically) using PET techniques. After ganciclovir treatment, only responding experimental tumors accumulated the radiolabeled tk-ligand [¹⁸F]FHBG (fluorohydroxymethylbutylguanine) on PET scans (Jacobs et al., 2007). Recently, and for the first time in humans, T-cells were marked with HSV1-tk, then infused into brain tumor patients and successfully imaged with [¹⁸F]FHBG-PET (Yaghoubi and Gambhir, 2009).

4. Conclusions and Future Perspectives

In summary, pharmacodynamic imaging end-points offer various basic, translational and clinical quantitative protocols which can be directly incorporated into multicenter trials (Evelhoch et al., 2005; Yankeelov et al., 2009). Multimodality approach will be one of the major technological investments in the future. The combination of molecular-functional-anatomic multiple imaging modalities will provide the highest advantage of non-invasive method because, as we could see above, each modality has its own strengths and weaknesses. The simplest way to obtain “multimodality” images is to acquire them at each modality separately and then, by applying an anatomic marker for co-registration, fuse the images using advanced imaging analysis software (Liao and Li, 2009). The “multimodal” platform can also be achieved by physically placing two modalities (a) adjunct to each other (for example, a docked PET/CT system with a moving animal bed from the PET into CT scanner); or (b) for a simultaneous acquisition, a hybrid scanner could be designed (for example, by placing PET rings inside of an MRI scanner) (de Kemp et al., 2010). The first multimodality platform, which has been introduced into the clinical setting in 2001, was a “docked” PET/CT system, followed in 2004 by SPECT/CT. In animal research, microPET/CT and microSPECT/CT (mostly based on the docked design) as well as a new generation of triple micro-PET/SPECT/CT scanners are using the high-resolution CT scan (with spatial resolution of the order of 100 microns) to “anatomically” adjust the functional images (PET and SPECT). However, the use of ionizing radiation from a high-resolution CT scanner is undesirable; moreover, CT scans provides anatomic localization only (Wagenaar et al., 2006). Most recently, the first attempts have been made both clinically and preclinically, to combine the two most sophisticated imaging modalities, namely PET and MRI. Several research groups used different approaches to integrate PET detectors into high-field MRI. Initially, systems were based on optical fibres guiding the scintillation light to the PET camera, which resides outside the fringe magnetic field. Recent advances in gamma ray detector technology paved the way towards the development of fully magnetic-field-insensitive high-performance PET detectors (Chaudhari et al., 2009). Combined PET/MRI

allows for multi-parametric imaging and will be, without any doubt, the modality of choice to obtain multiple functional and metabolic imaging end-points along with high-resolution morphology in cancer patients (Wehrl et al., 2009). In future PET/MRI scanners, the performance of all major MR applications, ranging from T1- or T2-weighted images up to echo-planar imaging (EPI) for functional (fMRI) as well as MRS, could be maintained when the PET insert was built into the MRI and acquiring PET data simultaneously. This obviously will be revolutionary while obtaining treatment end-points for metabolic activity (FDG-PET) with physiological read-outs (DCE-MRI or DW-MRI).

On the other hand, molecular imaging combines the disciplines of cell biology, molecular biology, synthetic chemistry and medical physics. In the future, it will be important to increase the sensitivity and specificity for the target while improving spatial resolution (multimodality PET/CT and PET/MRI). Development of new tracers with higher affinity for receptor proteins will help to distinguish the appropriate group of patients who will benefit of the receptor-inhibitor based therapies. Despite inconsistent clinical results in phase II/III gene therapy trials (Zeimet and Marth, 2003), gene transfer is still likely to have considerable potential to become an efficient anti-cancer treatment option. There are, however, many unanswered questions regarding the vector design. Molecular imaging can provide significant new information about the functionality and efficacy of current vector and gene delivery system. It is likely to aid the better design of local gene transfer methods and the selection and development of safe and efficient therapeutic genes.

There are various critical issues which need to be addressed for future success of functional and molecular imaging, which are related to (i) validation and quantification of imaging end-points; (ii) clinical trials of novel molecular imaging probes; (iii) the development of multi-modality platforms. Increasingly, oncologists envisage a time when cancers will be turned from life-threatening diseases into manageable chronic conditions. With novel therapeutics, combinations of drugs, the use of intelligent targets, and the development of biomarkers for treatment efficacy, one day truly individualized patient therapy may achieve that goal. Oncologic imaging of treatment response based on quantitative physiological, metabolic and molecular imaging read-outs has the potential to aid in that endeavor.

References

- Anderson CJ. ^{64}Cu -TETA-octreotide as a PET imaging agent for patients with neuroendocrine tumors. *J. Nucl. Med.* 2001; 42:213–221. [PubMed: 11216519]
- Artemov D, Mori N, Okollie B, Bhujwalla ZM. MR molecular imaging of the her-2/neu receptor in breast cancer cells using targeted iron oxide nanoparticles. *Magn. Reson. Med.* 2003; 49:403–408. [PubMed: 12594741]
- Barrett T, Brechbiel M, Bernardo M, Choyke PL. MRI of tumor angiogenesis. *J. Magn. Reson. Imag.* 2007; 26:235–249.
- Beer AJ, Grosu AL, Carlsen J, et al. [^{18}F]Galacto-RGD positron emission tomography for imaging of $\alpha\text{v}\beta 3$ expression on the neurovasculature in patients with squamous cell carcinoma of the head and neck. *Clin. Cancer Res.* 2007; 13:6610–6616. [PubMed: 18006761]
- Bisdas S, Medov L, Baghi M, et al. A comparison of tumor perfusion assessed by deconvolution-based analysis of dynamic contrast-enhanced CT and MR imaging in patients with squamous cell carcinoma of the upper aerodigestive tract. *Eur. Radiol.* 2008; 18:843–850. [PubMed: 18175123]
- Blodgett TM, Meltzer CC, Townsend DW. PET/CT: Form and function. *Radiology.* 2007; 242:360–385. [PubMed: 17255408]
- Blomley MJ, Eckersley RJ. Functional ultrasound methods in oncologic imaging. *Eur. J. Cancer.* 2002; 38:2108–2115. [PubMed: 12387836]
- Bolondi L, Correas JM, Lencioni R, Weskott HP, Piscaglia F. New perspectives for the use of contrast-enhanced liver ultrasound in clinical practice. *Dig. Liver Dis.* 2007; 39:187–195. [PubMed: 17208526]

- Brindle K. New approaches for imaging tumour responses to treatment. *Nat. Rev. Cancer*. 2008; 8:94–107. [PubMed: 18202697]
- Broxterman HJ, Gotink KJ, Verheul HM. Understanding the causes of multidrug resistance in cancer: a comparison of doxorubicin and sunitinib. *Drug Resist. Updates*. 2009; 12:114–126.
- Brunelle JK, Zhang B. Apoptosis assays for quantifying the bioactivity of anticancer drug products. *Drug Resist. Updates*. 2010; 13:172–179.
- Castell F, Cook GJ. Quantitative techniques in ^{18}F FDG-PET scanning in oncology. *Br. J. Cancer*. 2008; 98:597–560.
- Chang SK, Rizvi I, Solban N, Hasan T. In vivo optical molecular imaging of vascular endothelial growth factor for monitoring cancer treatment. *Clin. Cancer Res*. 2008; 14:4146–4153. [PubMed: 18593993]
- Chaudhari AJ, Joshi AA, Wu Y, Leahy RM, Cherry SR, Badawi RD. Spatial resolution correction and crystal identification for MRI-compatible position-sensitive avalanche photodiode-based PET scanners. *IEEE Trans. Nucl. Sci*. 2009; 56:549–556. [PubMed: 20161023]
- Dancey J, Sausville EA. Issues and progress with protein kinase inhibitors for cancer treatment. *Nat. Rev. Drug Discov*. 2003; 2:296–331. [PubMed: 12669029]
- De Kemp RA, Epstein FH, Catana C, Tsui BMW, Ritman EL. Small-animal molecular imaging methods. *J. Nucl. Med*. 2010; 51(Suppl 5):18S–32S. [PubMed: 20457793]
- Dent P, Curiel DT, Fisher PB, Grant S. *Drug Resist. Updates*. 2009; 12:65–73.
- Deppe MH, Parra-Robles J, Ajraou S, Wild JM. Combined measurement of pulmonary inert gas washout and regional ventilation heterogeneity by MR of a single dose of hyperpolarized ^3He . *Magn. Reson. Med*. 2011; 65:1075–1083. [PubMed: 21413071]
- Desouza NM, Reinsberg SA, Scurr ED, Brewster JM, Payne GS. Magnetic resonance imaging in prostate cancer: the value of apparent diffusion coefficient for identifying malignant nodules. *Br. J. Radiol*. 2007; 80:90–95. [PubMed: 17303616]
- Dobrucki L, de Muinck ED, Lindner JR, Sinusas AJ. Approaches to multimodality imaging of angiogenesis. *J. Nucl. Med*. 51 Suppl. 2010; 5:66S–79S.
- Druke BJ, Talpaz M, Resta DJ, et al. Efficacy and safety of a specific inhibitor of the BCR-ABL tyrosine kinase in chronic myeloid leukemia. *New Engl. J. Med*. 2001; 344:1031–1037. [PubMed: 11287972]
- Eisenhauer EA, Therasse P, Bogaerts J, Schwartz LH, Sargent D, Ford R, et al. New response evaluation criteria in solid tumours: Revised RECIST guideline (version 1.1). *Eur. J. Cancer*. 2009; 45:228–247. [PubMed: 19097774]
- Escudier B, Lassau N, Angevin E, Soria JC, Chami L, Lamuraglia M, et al. Phase I trial of sorafenib in combination with IFN alpha-2a in patients with unresectable and/or metastatic renal cell carcinoma or malignant melanoma. *Clin. Cancer Res*. 2007; 13:1801–1809. [PubMed: 17363536]
- Evelhoch J, Garwood M, Vigneron D, Knopp M, Sullivan D, Menkens A, Clarke L, Liu G. Expanding the use of magnetic resonance in the assessment of tumor response to therapy: workshop report. *Cancer Res*. 2005; 65:7041–7044. [PubMed: 16103049]
- Evilevitch V, Weber WA, Tap WD, et al. Reduction in glucose metabolic activity is more accurate than change in size at predicting histopathologic response to neoadjuvant therapy in high-grade soft-tissue sarcomas. *Clin. Cancer Res*. 2008; 14:715–720. [PubMed: 18245531]
- Folkman J. What is the evidence that tumors are angiogenesis dependent? *J. Nat. Cancer Inst*. 1990; 82:4–6. [PubMed: 1688381]
- Fueger BJ, Czernin J, Hilderbrandt I, Tran C, Halpern BS, Stout D, Phelps ME, Weber WA. Impact of animal handling on the results of ^{18}F -FDG-PET studies in mice. *J. Nucl. Med*. 2006; 47:999–1006. [PubMed: 16741310]
- Galbraith SM. MR in oncology drug development. *NMR Biomed*. 2006; 19:681–689. [PubMed: 16986117]
- Gambhir SS, Czernin J, Schwimmer J, et al. A tabulated summary of the FDG-PET literature. *J. Nucl. Med*. 2001; 42:1S–93S. [PubMed: 11483694]
- Gambhir SS. Molecular imaging of cancer with positron emission tomography. *Nat. Rev. Cancer*. 2002; 2:683–693. [PubMed: 12209157]

- Gillies RJ, Morse DL. *In vivo* magnetic resonance spectroscopy in cancer. *Annu. Rev. Biomed. Eng.* 2005; 7:287–326. [PubMed: 16004573]
- Granot D, Addadi Y, Kalchenko V, et al. *In vivo* imaging of the systemic recruitment of fibroblasts to the angiogenic rim of ovarian carcinoma tumors. *Cancer Res.* 2007; 67:9180–9189. [PubMed: 17909023]
- Greenbaum L, Burns P, Copel J, et al. American Institute of Ultrasound in Medicine recommendations for contrast-enhanced liver ultrasound imaging clinical trials. *J. Ultrasound Med.* 2007; 26:705–716. [PubMed: 17526602]
- Gregoire V, Haustermans K, Geets X, Roels S, Lonneux M. PET-based treatment planning in radiotherapy: A new standard? *J. Nucl. Med.* 2007; 48:68S–77S. [PubMed: 17204722]
- Halpern E. Contrast-enhanced ultrasound imaging of prostate cancer. *Rev. Urol.* 2006; 8:S29–S37. [PubMed: 17021624]
- Hasebroock KM, Serkova NJ. Toxicity of MRI and CT contrast agents. *Expert Opin. Drug Metab. Toxicol.* 2009; 5:403–416. [PubMed: 19368492]
- Henze M. PET imaging of somatostatin receptors using [⁶⁸Ga]DOTA-D-Phe-1-Tyr3-octreotide: First results in patients with meningiomas. *J. Nucl. Med.* 2001; 42:1053–1056. [PubMed: 11438627]
- Hogemann D, Josephson L, Weissleder R, Basilion JP. Improvement of MRI probes to allow efficient detection of gene expression. *Bioconj. Chem.* 2000; 11:941–946.
- Hollande F, Pannequin J, Joubert D. The long road to colorectal cancer therapy: searching for the right signals. *Drug Resist. Updates.* 2010; 13:44–56.
- Hughes B, Yip D, Goldstein D, et al. Cerebral relapse of metastatic gastrointestinal stromal tumor during treatment with imatinib mesylate: Case report. *BMC Cancer.* 2004; 4:1–7. [PubMed: 14725718]
- Hylton N. Dynamic contrast-enhanced magnetic resonance imaging as an imaging biomarker. *J. Clin. Oncol.* 2006; 24:3293–3298. [PubMed: 16829653]
- Jacobs AH, Rueger MA, Winkeler A, Li H, Vollmar S, Waerzeggers Y.M, et al. Imaging-guided gene therapy of experimental gliomas. *Cancer Res.* 2007; 67:1706–1715. [PubMed: 17308112]
- Jaffe CC. Measures of response: RECIST, WHO, and new alternatives. *J. Clin. Oncol.* 2006; 24:3245–3251. [PubMed: 16829648]
- Jaffe CC. Response assessment in clinical trials: Implications for sarcoma clinical trial design. *Oncologist.* 2008; 13:14–18. [PubMed: 18434633]
- Jain RK. Molecular regulation of vessel maturation. *Nat. Med.* 2003; 9:685–693. [PubMed: 12778167]
- Kapoor V, Fukui MB, McCook BM. Role of ¹⁸F-FDG PET/CT in the treatment of head and neck cancers: Principles, technique, normal distribution, and initial staging. *AJR Am. J. Roentgenol.* 2005a; 184:579–587. [PubMed: 15671384]
- Kapoor V, Fukui MB, McCook BM. Role of ¹⁸F-FDG PET/CT in the treatment of head and neck cancers: posttherapy evaluation and pitfalls. *AJR Am. J. Roentgenol.* 2005b; 184:589–597. [PubMed: 15671385]
- Kerbel RS, Kamen BA. The anti-angiogenic basis of metronomic chemotherapy. *Nat. Rev. Cancer.* 2004; 4:423–436. [PubMed: 15170445]
- Koh DM, Collins DJ. Diffusion-weighted MRI in the body: Application and challenges in oncology. *Am. J. Roentgenol.* 2007; 188:622–635. [PubMed: 17312045]
- Kostakoglu L, Goldsmith SJ. PET in the assessment of therapy response in patients with sarcoma of the head and neck and of the esophagus. *J. Nucl. Med.* 2004; 45:56–68. [PubMed: 14734674]
- Kostakoglu L, Goldsmith SJ, Leonard JP, et al. FDG-PET after cycle 1 of therapy predicts outcome in diffuse large cell lymphoma and classic Hodgkin disease. *Cancer.* 2006; 107:2678–2687. [PubMed: 17063502]
- Krause BJ, Souvatzoglou M, Treiber U. Imaging of prostate cancer with PET/CT and radioactively labeled choline derivatives. *Urol. Oncol.* 2011 Mar 7 [Epub ahead of print].doi:10.1016/j.urolonc.2010.08.008.
- Kurhanewicz J, Vigneron DB, Brindle K, Chekmenev EY, Comment A, Cunningham CH. Analysis of cancer metabolism by imaging hyperpolarized nuclei: prospects for transition to clinical research. *Neoplasia.* 2011; 13:81–97. [PubMed: 21403835]

- Lamuraglia M, Escudier B, Vhami L, Schwartz B, Leclere J, Roche A, Lassau N. To predict progression-free survival and overall survival in metastatic renal cancer treated with sorafenib: pilot study using contrast-enhanced Doppler ultrasound. *Eur. J. Cancer.* 2006; 42:2472–2479. [PubMed: 16965911]
- Lassau N, Lamuraglia M, Chami L, Leclere J, Bonvalot S, Terrier P, Roche A, Le Cesne A. Gastrointestinal stromal tumors treated with imatinib: monitoring response with contrast-enhanced sonography. *Am. J. Roentgenol.* 2006; 187:1267–1273. [PubMed: 17056915]
- Lassau N, Chami L, Benatsou B, Peronneau P, Roche A. Dynamic contrast-enhanced ultrasonography (DCE-US) with quantification of tumor perfusion: a new diagnostic tool to evaluate the early effects of antiangiogenic treatment. *Eur. Radiol. Suppl.* 2007; 17:F89–F98.
- Lauterbur PC. Nobel Lecture: All science is interdisciplinary – from magnetic moments to molecules to men. *Biosci. Rep.* 2004; 24:165–178. [PubMed: 16209126]
- Leach MO, Brindle KM, Evelhoch JL, et al. The assessment of antiangiogenic and antivascular therapies in early-stage clinical trials using magnetic resonance imaging: issues and recommendations. *Br. J. Cancer.* 2005; 92:1599–1610. [PubMed: 15870830]
- Leach MO. Magnetic resonance spectroscopy (MRS) in the investigation of cancer at The Royal Marsden Hospital and The Institute of Cancer Research. *Phys. Med. Biol.* 2006; 51:R61–R82. [PubMed: 16790921]
- Leibold T, Akhurst TJ, Chessin DB, et al. Evaluation of 18F-FDG-PET for early detection of suboptimal response of rectal cancer to perioperative chemoradiotherapy: a prospective analysis. *Ann. Surg. Oncol.* 2011 Apr 8 [Epub ahead of print].doi:10.1245/s10434-011-1634-2.
- Levitzi A, Gazit A. Tyrosine kinase inhibition: an approach to drug development. *Science.* 1995; 267:782–728. [PubMed: 17813884]
- Leyton J, Latigo JR, Perumal M, et al. Early detection of tumor response to chemotherapy by 3-deoxy-3-[¹⁸F]fluorothymidine positron emission tomography: the effect of cisplatin on a fibrosarcoma tumor model in vivo. *Cancer Res.* 2005; 65:2005–2010.
- Liao AH, Li PC. The role of high-frequency ultrasound in multimodality small animal imaging for cancer research. *J. Med. Ultrasound.* 2009; 17:86–97.
- Lippert TH, Ruoff HJ, Volm M. Current status of methods to assess cancer drug resistance. *Int. J. Med. Sci.* 2011; 23:245–253. [PubMed: 21487568]
- Liu G, Rugo HS, Wilding G, et al. Dynamic contrast-enhanced magnetic resonance imaging as a pharmacodynamic measure of response after acute dosing of AG-013736, an oral angiogenesis inhibitor, in patients with advanced solid tumors: results from a phase I study. *J. Clin. Oncol.* 2005; 23:5464–5473. [PubMed: 16027440]
- Mansfield P. Snapshot magnetic resonance imaging (Nobel lecture). *Angew. Chem. Int. Ed. Engl.* 2004; 43:5456–5464. [PubMed: 15384128]
- Marzola P, Degrassi A, Calderan L, et al. *In vivo* assessment of antiangiogenic activity of SU6668 in an experimental colon carcinoma model. *Clin. Cancer Res.* 2004; 10:739–750. [PubMed: 14760097]
- Massoud TF, Gambhir SS. Molecular imaging in living subjects: seeing fundamental biological processes in a new light. *Genes Develop.* 2003; 17:545–580. [PubMed: 12629038]
- McSheehy PMJ, Weidensteiner C, Cannet C, et al. Quantified tumor T1 is a generic early-response imaging biomarker for chemotherapy reflecting cell viability. *Clin. Cancer Res.* 2009; 16:212–225. [PubMed: 20008843]
- Miles KA, Young H, Chica SL, Esser PD. Quantitative contrast-enhanced computed tomography: is there a need for system calibration? *Eur. Radiol.* 2007; 17:919–926. [PubMed: 17008987]
- Mileshkin L, Hicks RJ, Hughes BG, et al. Changes in FDG- and FLT-PET imaging in patients with non-small cell lung cancer treated with erlotinib. *Clin. Cancer Res.* 2011 2011 Mar 1 [Epub ahead of print].doi:10.1158/1078-0432.CCR-10-2763.
- Moasser MM, Wilmes LJ, Wong CH, et al. Improved vascular function following high-dose epidermal growth factor receptor tyrosine kinase inhibitor therapy. *J. Magn. Reson. Imag.* 2007; 26:1618–1625.
- Morgan B, Thomas AL, Dreves J, et al. Dynamic contrast-enhanced magnetic resonance imaging as a biomarker for the pharmacological response of PTK787/ZK 222584, an inhibitor of the vascular

- endothelial growth factor receptor tyrosine kinases, in patients with advanced colorectal cancer and liver metastases: results from two Phase I studies. *J. Clin. Oncol.* 2003; 21:3955–3964. [PubMed: 14517187]
- Na II, Byun BH, Kang HJ, et al. ¹⁸F-Fluoro-2-deoxy-glucose uptake predicts clinical outcome in patients with gefitinib-treated non-small cell lung cancer. *Clin. Cancer Res.* 2008; 14:2036–2041. [PubMed: 18381942]
- Nagengast WB, Lub-de Hooge MN, Oosting SF, et al. VEGF-PET Imaging is a noninvasive biomarker showing differential changes in the tumor during sunitinib treatment. *Cancer Res.* 2011; 71:143–153. [PubMed: 21084271]
- Nahta R, Esteva RJ. Trastuzumab: triumphs and tribulations. *Oncogene.* 2007; 26:3637–3643. [PubMed: 17530017]
- Nayak TK, Garmestani K, Milenic DR, et al. HER1-targeted Y-panitumumab possesses superior targeting characteristics than Y-cetuximab for PET imaging of human malignant mesothelioma tumors xenografts. *PLoS One.* 2011; 6:e18198. [PubMed: 21464917]
- Ott K, Herrmann K, Lordick F, et al. Early metabolic response evaluation by fluorine-18 fluorodeoxyglucose positron emission tomography allows in vivo testing of chemosensitivity in gastric cancer: long-term results of a prospective study. *Clin. Cancer Res.* 2008; 14:2012–2018. [PubMed: 18381939]
- Padhani AR, Harvey CJ, Cosgrove DO. Angiogenesis imaging in the management of prostate cancer. *Nat. Clin. Pract. Urol.* 2005; 2:596–607. [PubMed: 16474547]
- Padhani AR, Liu G, Koh DM, et al. Diffusion-weighted magnetic resonance imaging as a cancer biomarker: consensus and recommendations. *Neoplasia.* 2009; 11:102–125. [PubMed: 19186405]
- Pope WB, Young JR, Ellingson BM. Advances in MRI assessment of gliomas and response to anti-VEGF therapy. *Curr. Neurol. Neurosci. Rep.* 2011; 11:336–344. [PubMed: 21234719]
- Pucar D, Shukla-Dave A, Hricak H, et al. Prostate cancer: correlation of MR imaging and MR spectroscopy with pathologic findings after radiation therapy – Initial experience. *Radiology.* 2005; 236:545–553. [PubMed: 15972335]
- Pucar D, Sella T, Schroder H. The role of imaging in the detection of prostate cancer local recurrence after radiation therapy and surgery. *Curr. Opin. Urol.* 2008; 18:87–97. [PubMed: 18090496]
- Ramasamy K, Nield L, Serkova NJ, Hasebroock KM, Tyagi A, Raina K, et al. Silibinin prevents lung tumorigenesis in wild-type but not in iNOS^{-/-} mice: potential of real-time microCT in lung cancer chemoprevention studies. *Clin. Cancer Res.* 2011; 17:753–761. [PubMed: 21148748]
- Reinsberg SA, Payne GS, Riches SF, et al. Combined use of diffusion-weighted MRI and ¹H-MR spectroscopy to increase accuracy in prostate cancer detection. *Am. J. Roentgenol.* 2007; 188:91–98. [PubMed: 17179350]
- Robinson SP, McIntyre DJO, Checkley D, et al. Tumor dose response to the antivascular agent ZD6126 assessed by magnetic resonance imaging. *Br. J. Cancer.* 2003; 88:1592–1597. [PubMed: 12771928]
- Rozel S, Galban CJ, Nicolay K, et al. Synergy between anti-CCL2 and docetaxel as determined by DW-MRI in a metastatic bone cancer model. *J. Cell. Biochem.* 2009; 107:58–64. [PubMed: 19259948]
- Semple SIK, Staff RT, Heys SD, et al. Baseline MRI delivery characteristics predict change in invasive ductal breast carcinoma PET metabolism as a result of primary chemotherapy administration. *Ann. Oncol.* 2006; 17:1393–1398. [PubMed: 16788001]
- Serkova NJ, Garg K, Bradshaw-Pierce EL. Oncologic imaging end-points for the assessment of therapy response. *Recent Pat. Anticancer Drug Discov.* 2009; 4:36–53. [PubMed: 19149687]
- Serkova NJ, Renner B, Larsen BA, Stoldt CR, Hasebroock KM, Bradshaw-Pierce EL, Holers VM, Thurman JM. Renal inflammation: targeted iron oxide nanoparticles for molecular MR imaging in mice. *Radiology.* 2010; 255:517–526. [PubMed: 20332377]
- Shanka LK, Hoffman JM, Bacharach S, et al. Consensus recommendations for use of ¹⁸F-FDG PET as an indicator of therapeutic response in patients in National Cancer Institute trials. *J. Nucl. Med.* 2006; 47:1059–1066. [PubMed: 16741317]
- Siemerink EJ, Mulder NH, Brouwers AH, Hospers GAP. ¹⁸F-Fluorodeoxyglucose positron emission tomography for monitoring response to sorafenib treatment in patients with hepatocellular carcinoma. *Oncologist.* 2008; 13:734–735. [PubMed: 18586929]

- Spratlin JL, Cohen RB, Eadens M, et al. Phase I pharmacologic and biologic study of Ramucirumab (IMC-1121B), a fully human immunoglobulin G₁ monoclonal antibody targeting the vascular endothelial growth factor receptor-2. *J. Clin. Oncol.* 2010; 28:780–787. [PubMed: 20048182]
- Su H, Bodenstern C, Dumont RA, et al. Monitoring tumor glucose utilization by positron emission tomography for the prediction of treatment response to epidermal growth factor receptor kinase inhibitor. *Clin. Cancer Res.* 2006; 12:5659–5667. [PubMed: 17020967]
- Therasse P, Arbuck SG, Eisenhauer EA, Wanders J, Kaplan RS, Rubinstein L, et al. New guidelines to evaluate the response to treatment in solid tumors. European Organization for Research and treatment of Cancer, National Cancer Institute of the United States, National Cancer Institute of Canada. *J. Natl. Cancer Inst.* 2000; 92:205–216. [PubMed: 10655437]
- Thoeny HC, Ross BD. Predicting and monitoring treatment response with diffusion-weighted MRI. *J. Magn. Reson. Imaging.* 2010; 32:2–16. [PubMed: 20575076]
- Thomassin-Naggara I, Bazot M, Darai E, et al. Epithelial ovarian tumors: values of dynamic contrast-enhanced MR imaging and correlation with tumor angiogenesis. *Radiology.* 2008; 248:148–159. [PubMed: 18458244]
- Tidwell AS, Jones JC. Advanced imaging concepts: A pictorial glossary of CT and MRI technology. *Clin. Tech. Small Anim. Pract.* 1999; 14:65–111. [PubMed: 10361360]
- Troiani T, Serkova NJ, Gustafson DL, et al. Investigation of two dosing schedules of Vandetanib (ZD6474), an inhibitor of VEGFR and EGFR signaling, in combination with Irinotecan in a human colon cancer xenograft model. *Clin. Cancer Res.* 2007; 13:6450–6458. [PubMed: 17975157]
- Turnbull LW. Dynamic contrast-enhanced MRI in the diagnosis and management of breast cancer. *NMR Biomed.* 2009; 22:28–39. [PubMed: 18654999]
- Vaughan CL, Mayosi BM. Origins of computed tomography. *Lancet.* 2007; 369:1168. [PubMed: 17416259]
- Wagenaar DJ, Kapusta M, Li J, Patt BE. Rationale for the combination of nuclear medicine with magnetic resonance for pre-clinical imaging. *Technol. Cancer Res. Treat.* 2006; 5:343–350. [PubMed: 16866565]
- Weber WA. Use of PET for monitoring cancer therapy and for predicting outcome. *J. Nucl. Med.* 2005; 46:983–995. [PubMed: 15937310]
- Weber W, Figlin R. Monitoring cancer treatment with PET/CT: Does it make a difference? *J. Nucl. Med.* 2007; 48:36S–44S. [PubMed: 17204719]
- Wehrli HF, Judenhofer MS, Wiehr S, Pichler BJ. Pre-clinical PET/MRI: technological advances and new perspectives in biomedical research. *Eur. J. Nucl. Med. Mol. Imaging.* 2009; 36(Suppl 1):S56–S68. [PubMed: 19194703]
- Weissleder R, Mahmood U. Molecular imaging. *Radiology.* 2001; 219:316–333. [PubMed: 11323453]
- Weissleder R, Ntziachristos V. Shedding light into blive molecular targets. *Nat. Med.* 2003; 9:123–128. [PubMed: 12514725]
- Wilson SR, Greenbaum LD, Goldberg BB. Contrast-enhanced ultrasound: what is the evidence and what are the obstacles? *Am. J. Roentgen.* 2009; 193:55–60.
- Wilson SR, Burns PN. Microbubble-enhanced US in body imaging: what role? *Radiology.* 2010; 257:24–39. [PubMed: 20851938]
- Yaghoubi S, Gambhir S. Nature Clinical Practice Oncology 2008. *Nat. Clin. Pract. Oncol.* 2009; 6:53–58. [PubMed: 19015650]
- Yankeelov TE, Avison MJ, Damon BM, Manning HC, Peterson TE, Gore JC. Frontiers of biomedical imaging science 2009: workshop report and research opportunities. *Cancer Res.* 2009; 69:7902–7904. [PubMed: 19808955]
- Zahara MA, Hollingsworth KG, Sala E, Lomas DJ, Tan LT. Dynamic contrast-enhanced MRI as a predictor of tumor response to radiotherapy. *Lancet Oncol.* 2007; 8:63–74. [PubMed: 17196512]
- Zander T, Scheffler M, Nogova L, et al. Early prediction of nonprogression in advanced non-small-cell lung cancer treated with erlotinib by using 18F-fluorodeoxyglucose and 18F-fluorothymidine positron emission tomography. *J. Clin. Oncol.* 2011 Mar 21 [Epub ahead of print].doi: 10.1200/JCO.2010.32.4939.

- Zeimet AG, Marth C. Why did p53 gene therapy fail in ovarian cancer? *Lancet Oncol.* 2003; 4:415–422. [PubMed: 12850192]
- Zhang S, Huang WC, Li P, Guo H, Poh SB, Brady SW, et al. Combating trastuzumab resistance by targeting SRC, a common node downstream of multiple resistance pathways. *Nat. Med. Publ.* 2011 online 13 march 2011; doi:10.1038/nm.2309.
- Zhang X, Lin Y, Gillies RJ. Tumor pH and its measurement. *J. Nucl. Med.* 2010; 51:1167–1170. [PubMed: 20660380]

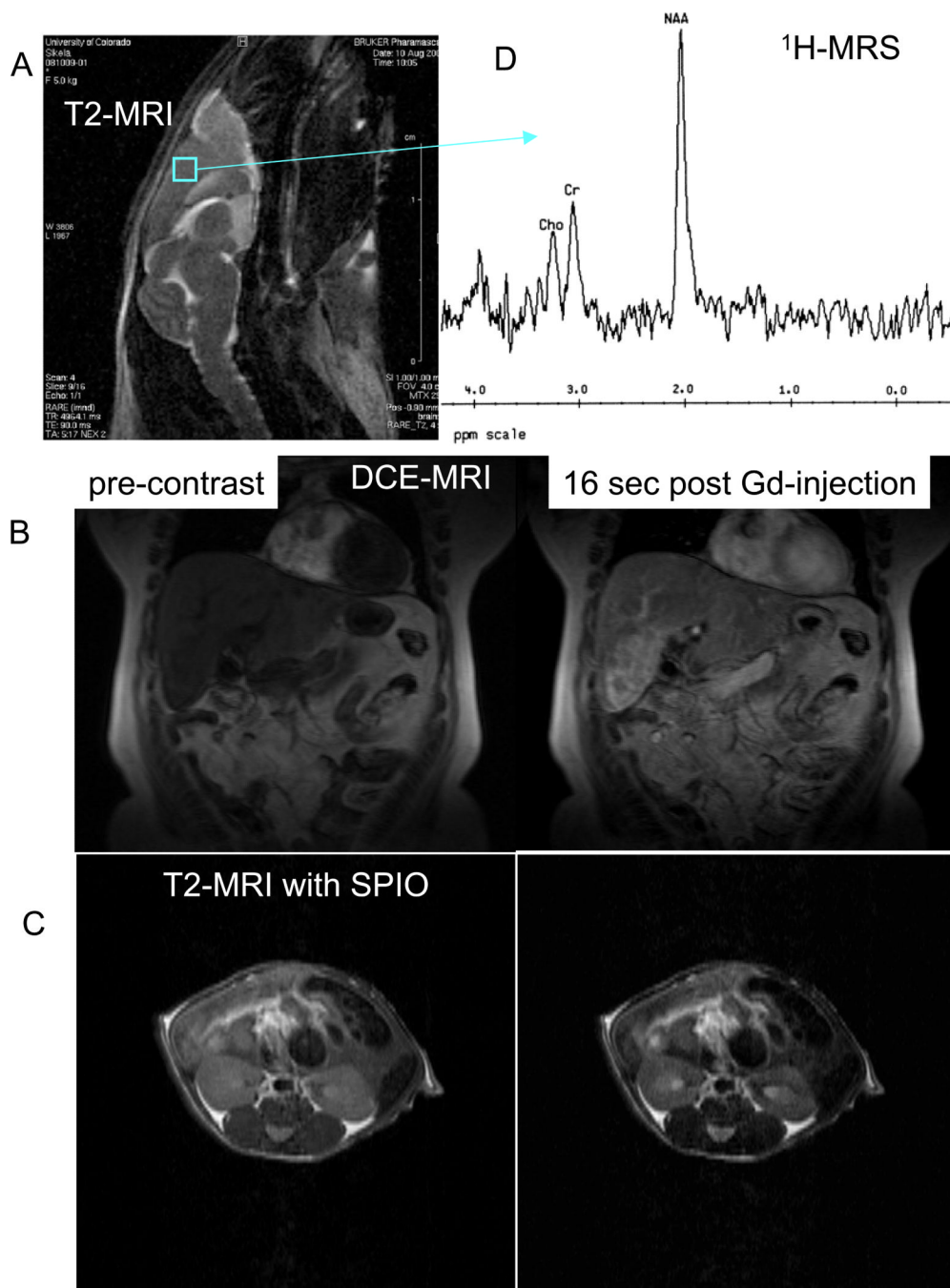


Figure 1. Magnetic resonance images and spectra. (A) Anatomical T2-weighted MRI of mouse brain; (B) dynamic contrast-enhanced (DCE) MRI on a patient with liver metastasis (before and 16 seconds after bolus gadolinium injection); (C) T2-weighted images of mouse kidneys before and after injection of targeted super paramagnetic iron oxide nanoparticles (SPIO); (D) proton (^1H) MRS on mouse brain.

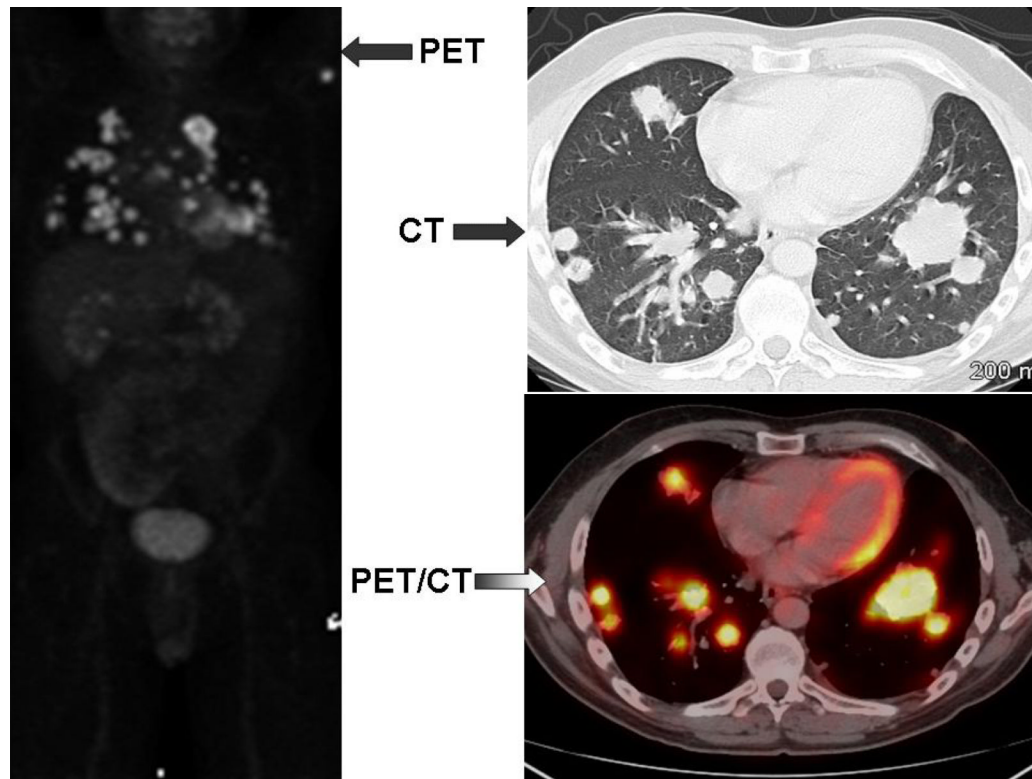


Figure 2. PET, chest CT and fused PET/CT images on a patient with multiple pulmonary metastasis from colon cancer.

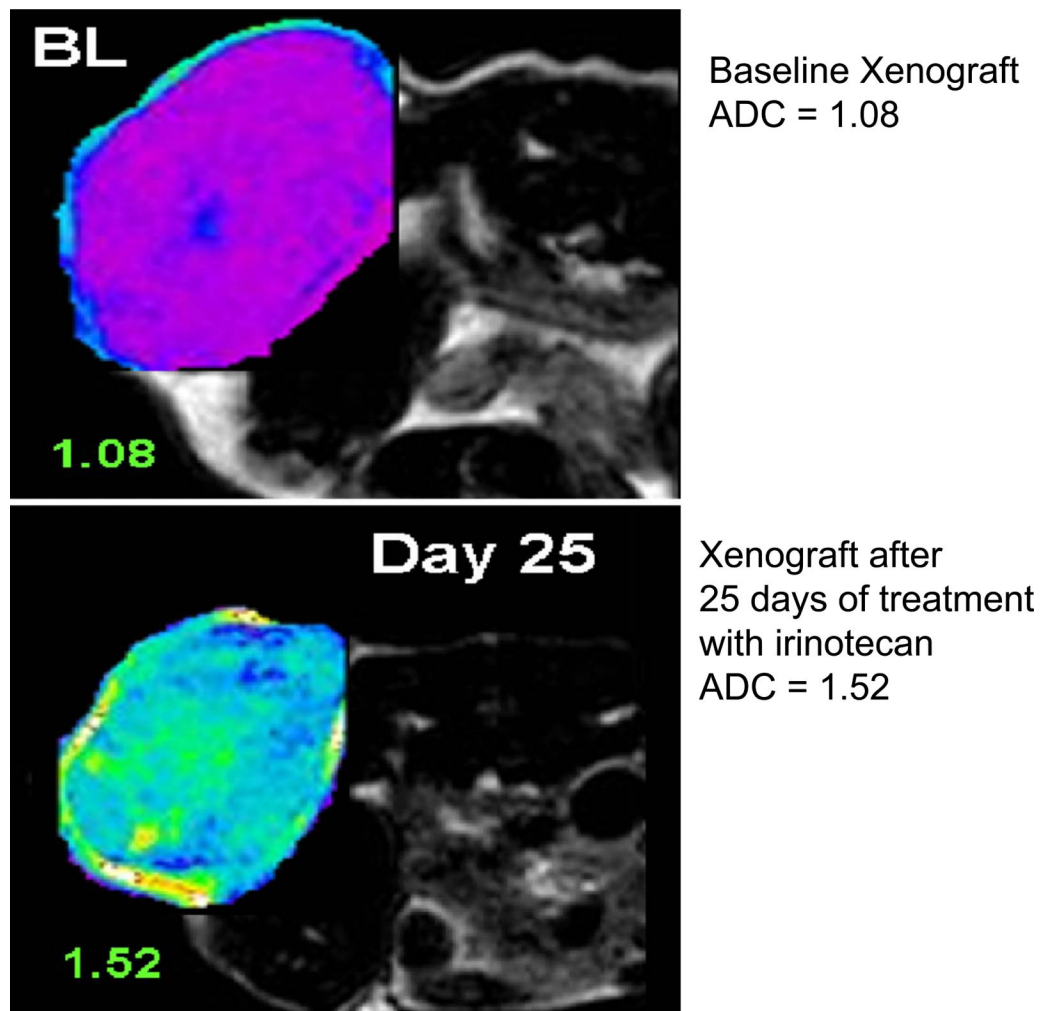


Figure 3. Diffusion-weighted (DW) MRI on nude mouse implanted with human colorectal cancer (CRC) cells (xenografts). Apparent diffusion coefficient (ADC) increases after 25 days of treatment with irinotecan (a chemotherapeutic agent) indicating decrease cellularity and induction of apoptosis.

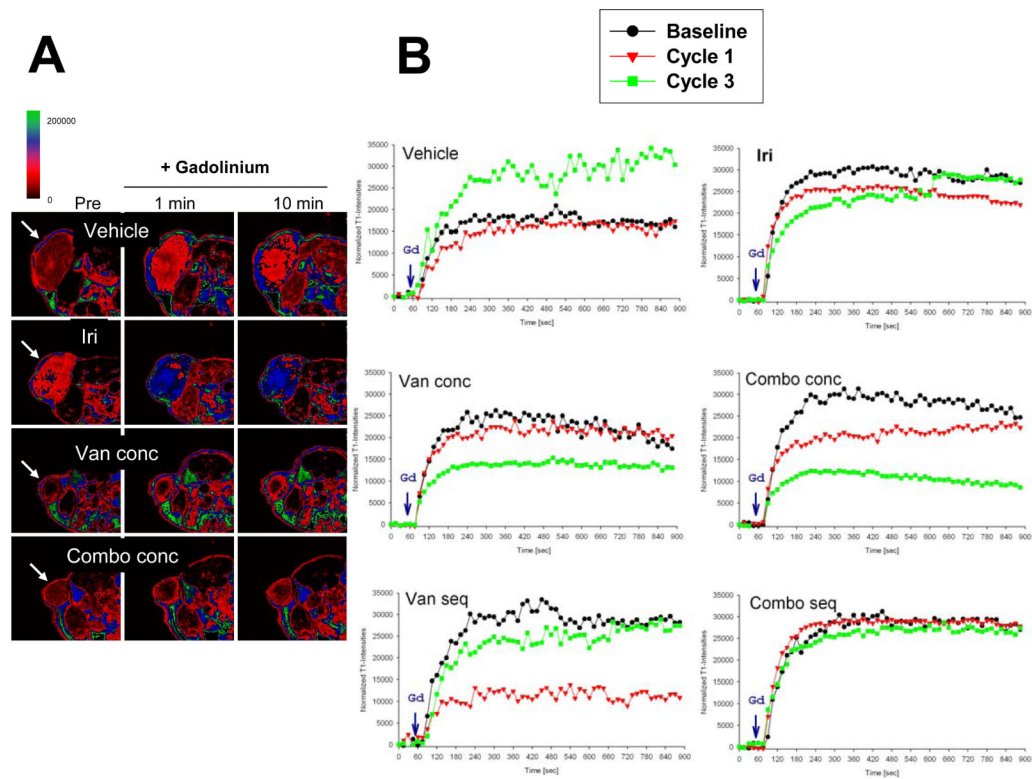


Figure 4.

Dynamic contrast-enhanced magnetic resonance imaging (DCE-MRI) analysis on mouse CRC xenografts. A) T1 weighted images prior (pre) and after 0.1 mmol/kg gadodiamide injection (1 min and 10 min) of a representative tumor from control and various treatment groups (including irinotecan, the VEGFR2 tyrosine kinase inhibitor vandetanib and their combination). B) Normalized T1-intensity curves in tumors before (baseline, black circles), after 10 days (Cycle 1, red triangles) and 30 days (Cycle 3, green squares) of treatment (adapted from Troiani, Serkova et al., 2007). Abbreviations: combo, combination treatment with irinotecan and vandetanib; conc, concurrent treatment with irinotecan and vandetanib; Iri, irinotecan; seq, sequential treatment with irinotecan and vandetanib; Van, vandetanib.

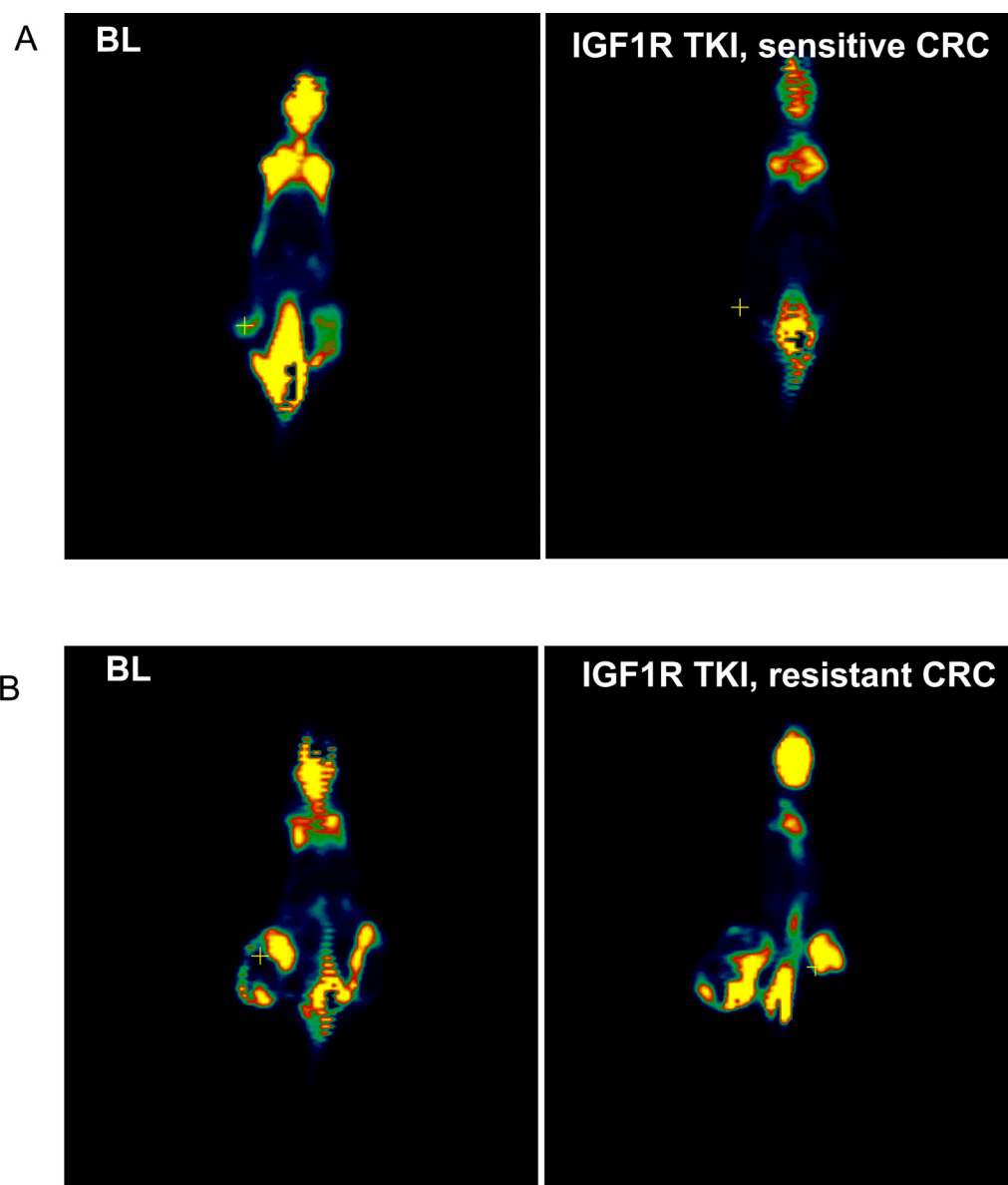


Figure 5. ^{18}F -Fluoroseoxyglucose (FDG) PET of mouse CRC xenografts treated with an IGF1R tyrosine kinase inhibitor (TKI) at the baseline (BL) and 14 days after treatment (A) responder and (B) non-responder.

Table 1

Major Advantages and Disadvantages of Imaging Modalities in Human and Animal Imaging.

Modality	Resolution [mm]		Specificity/Sensitivity	Anatomic Potential	Functional Potential	Molecular Potential
	Clinical	Research				
MRI	5	0.1	high	excellent	excellent	high
CT	5	0.05	high-moderate	excellent	moderate	low
SPECT	10-15	1.5-2	moderate-high	moderate	moderate	high-moderate
PET	10-15	1.5-2	high-excellent	moderate	excellent	high
Ultrasound	5-10	0.2-0.5	moderate	High-moderate	high	moderate-low
Optical	N/A	(0.5)	excellent	moderate-low	moderate	excellent